Planta (2002) 215: 67–78
DOI 10.1007/s00425-002-0746-0

ORIGINAL ARTICLE

Sandra Ormenese · Andrée Havelange · Georges Bernier
Chris van der Schoot

The shoot apical meristem of *Sinapis alba* L. expands its central symplasmic field during the floral transition

Received: 26 July 2001 / Accepted: 14 January 2002 / Published online: 13 March 2002

Abstract The shoot apical meristem (SAM) is functionally subdivided into zones with distinct tasks. During vegetative growth the peripheral zone of the meristem gives rise to leaf primordia that develop into dorsiventral leaves under the influence of signals from the central zone. During the floral transition the function of the SAM is altered and its peripheral zone starts to form floral structures in a specific pattern. This requires alterations in the signal networks that coordinate the activities of the peripheral and central zone of the SAM. These signal networks are partly housed in the symplasmic space of the SAM. Dye-coupling experiments demonstrate that in the superficial layer of the *Sinapis alba* meristem this space is radially subdivided. The cells of the central zone are coupled into a symplasmic field, which is shielded from the peripheral zone by the positional closing of plasmodesmata. In the vegetative meristems, most of these central symplasmic fields have a triangular geometry and are relatively small in size. Plants that are induced to flower by exposure to a single long day alter the geometry as well as the size of their central symplasmic field. After two subsequent days under short photoperiod the central symplasmic fields exhibit a circular form. Simultaneously, their size strongly increases both in an absolute sense and relative to the enlarging meristem. The geometric change in the fields is hypothesized to be due to recruitment of extra initial cells, required to support the increase in phyllotactic complexity. The proportional increase in field size is interpreted as an adjustment in the balance between the central and peripheral zone of the SAM, accompanying the shift from leaf production to flower formation.

Keywords Central zone (shoot apex) · Floral transition · Plasmodesmata · Shoot apical meristem · *Sinapis* (flowe- ring) · Central symplasmic field

Abbreviations B: blue light · BV: blue-violet light · CSF: central symplasmic field · E_m: membrane potential · GFP: green fluorescent protein · *h*: height of the shoot apical meristem dome · LD: long day · LYCH: Lucifer Yellow CH · *P*: surface area of the central symplasmic field as a proportion of the total surface area of the shoot apical meristem dome · Pd: plasmodesmata · *r*: radius of the shoot apical meristem dome · *S*: surface area of the projected central symplasmic field · SAM: shoot apical meristem · SD: short day · SEL: size exclusion limit

Introduction

In higher plants the shoot apical meristem (SAM) gives rise to the entire shoot system. At a later stage of the life cycle in annual plants, depending on environmental conditions and/or endogenous cues, the SAM embarks on a route to floral transition and starts forming an inflorescence or a single flower. In many plant species this morphogenetic shift from vegetative to reproductive functioning is accompanied by distinct changes at various levels of SAM organization (Bernier 1989; Lyndon 1998).

In vegetatively developing plants the SAM is often dome-shaped, and it consists of a small number of relatively undifferentiated and dividing cells, the outer of which are arranged in layers. Commonly, two external cell layers (L1 and L2) form a tunica, an expanding sheet

S. Ormenese · A. Havelange · G. Bernier
Laboratoire de Physiologie,
Département de Biologie végétale,
Université de Liège, Sart-Tilman,
4000 Liège, Belgium

C. van der Schoot (✉)[1]
ATO, Bornsesteeg 59, P.O. Box 17,
6700 AA Wageningen, The Netherlands

Present address:
[1]Plant Developmental Physiology,
Department of Biology & Nature Conservation,
Agricultural University of Norway,
P.O. Box 5014, 1432 Aas, Norway
(e-mail: chris.vanderschoot@ibn.nlh.no,
Fax: +47-6494-8502)

of cells that is maintained by anticlinal cell divisions (perpendicular to the SAM surface). Periclinal divisions (parallel to the SAM surface) can occur, however, and they are particularly frequent in the L2 at locations where leaf primordia arise. The corpus below the tunica constitutes a body of cells that divide in all planes. The tunica of the SAM is responsible for surface growth, whereas the cell divisions in the corpus increase the volume of the SAM. Although the cells of the corpus are normally not arranged in layers, they may be collectively referred to as L3. A cytohistological zonation is usually present across this layered structure, and is microscopically visible in the differential staining of the periphery and the centre of the SAM. Zonation correlates with cellular parameters, for example, the cells of the central zone in the tunica as well as the corpus divide less frequently and have a smaller amount of RNA and protein than the cells of the peripheral zone (Nougarède 1967; Steeves and Sussex 1989; Lyndon 1998). These and other cytohistological and cell kinetic differences between zones of the SAM suggest the existence of internal physiological barriers that isolate physiologically united central-zone cells from the more active cells around them laterally and basally (Sawhney et al. 1981).

In general, metabolic and physiological coupling is present when cells are well interconnected by open plasmodesmata (Pd; Lucas et al. 1993). The cells of the SAM appeared to be interconnected structurally by numerous Pd (e.g. Bergmans et al. 1997; Ormenese et al. 2000). In addition, it has been shown that these Pd are functional, and that positionally determined diffusion barriers exist within this network, giving rise to symplasmic fields that correspond to the cytohistological zones (Rinne and van der Schoot 1998; van der Schoot and Rinne 1999a, b; Gisel et al. 1999; Rinne et al. 2001). Symplasmic fields might not only serve metabolic coupling of SAM cells, but also the exchange of morphogens that are involved in the coordination of cell activities (Rinne and van der Schoot 1998). For example, Pd within symplasmic fields not only permit the proper distribution of metabolites, but also of important ions, hormones, and other signaling molecules such as inositol-1,4,5-triphosphate and cAMP, which diffuse along their chemical gradient from cell to cell. This suggests that small diffusing molecules and signals are channeled within the SAM in well-defined cytohistological areas where cells are coupled into symplasmic fields. Symplasmic fields are important in morphogenesis, as demonstrated by their alteration during morphogenetic switching in, for example, dormancy cycling. In birch seedlings the symplasmic fields dissipate under a short photoperiod – yielding a collection of symplasmically isolated cells in an endodormant SAM (Rinne and van der Schoot 1998). Restoration of these fields by the chilling effect of winter breaks dormancy and prepares the SAM for renewed development (Rinne et al. 2001).

Evidence is emerging that, in addition to small signaling molecules, certain proteins can also move within the meristem. For example, the homeodomain protein KNOTTED1 (a transcription factor) is found in the tunica of the maize SAM, although its RNA is not present (Jackson et al. 1994; Lucas et al. 1995). Mosaic studies have shown that some floral transcription factors, like GLOBOSA and DEFICIENS, and FLORICAULA, can move within the SAM of *Antirrhinum* (Perbal et al. 1996) and *Arabidopsis* (Carpenter and Coen 1995; Hantke et al. 1995), respectively. Recently, Sessions et al. (2000) showed that LEAFY protein, when expressed in a sector of a mutant, could restore the wild-type phenotype. This demonstrated that the protein not only moved within the SAM, inside and across layers, but also that it was fully functional. Although it was not shown through which paths the protein traffics, it seems very likely that it moves symplasmically via Pd. Although LEAFY moves in all directions in the meristem (Sessions et al. 2000), most other transcription factors move from layer to layer and show very restricted movement in the lateral direction. Movement of transcription factors may have important implications for the orchestration of normal developmental events at the SAM, particularly if they traffic selectively to certain areas.

Combination of the data on cytohistological zonation, symplasmic fields, and macromolecular movement inside the SAM leads to the conclusion that positional closing of Pd at the boundaries of the symplasmic fields safeguards the existence of groups of cells that share their metabolism and, for example, cell cycling rates, whereas coordination between these groups is achieved via macromolecular trafficking (for a model, see van der Schoot and Rinne 1999b). The Pd at the field boundaries must therefore be 'gatable' in order to allow passage of macromolecular factors (Crawford and Zambryski 1999; van der Schoot and Rinne 1999a, b). Recently, it has been shown that Pd in sink areas are dilated to the extent that green fluorescent protein (GFP)-fusion proteins can move through by simple diffusion (Imlau et al. 1999; Oparka et al. 1999; Crawford and Zambryski 2001). Whether such 'non-targeted' diffusional macromolecular transport occurs *within* symplasmic fields remains to be established, but it is unlikely to happen *across* field boundaries. Proteins that move everywhere in the meristem, like LEAFY, might therefore traffic through Pd that are gated after targeting by themselves or by a helper molecule.

During the floral transition the layered structure and the tunica/corpus organization are maintained, but the size and shape of the SAM are commonly profoundly altered. In addition, the cytohistological zonation may fade away and in some plants disappear altogether (Nougarède 1967; Lyndon 1998). The coordination of cell cycling in the SAM is markedly affected as shown by the overall increase in the rate of cell cycling and the partial synchronization of cell cycling (Bernier 1989). There is also a profound change in the pattern of gene activity with some genes up-regulated and others down-regulated at specific times during the transition, and in

specific areas of the SAM (Hempel et al. 1997; Kania et al. 1997; Ratcliffe et al. 1999; Hartmann et al. 2000; Samach et al. 2000). The change in output of the transitioning SAM involves the establishment of a new relation between the central and peripheral zone of the SAM. Morphologically this new relation is expressed in the production of a novel type of appendage and a change in phyllotactic pattern.

Although it seems likely that symplasmic alterations accompany this transition, this has not been a topic of thorough investigation. In an early study of the long-day (LD) plant *Silene coeli-rosa*, the spread of microinjected dyes within the SAM was reduced when it transformed into a terminal flower (Goodwin and Lyndon 1983), and in *Iris* a large group of cytoplasmically coupled cells broke up into subfields when the inflorescence meristem formed floral meristems (Bergmans et al. 1993). The experimental difficulties encountered during microinjection of delicate meristems, particularly in *Arabidopsis*, have encouraged the search for alternative methods. For example, 8-hydroxypyrene-1,3,6-trisulfonic acid (HPTS)-acetate was fed via the cut ends of petioles into the shoot system of *Arabidopsis*, and subsequent 'ester-loading' of the symplasmic space was followed by dye import into the SAM (Gisel et al. 1999). Dyes appeared to be excluded from the SAM at the time the plants were committed to flowering, suggesting a temporal cessation of dye import (Gisel et al. 1999). This indicates that the meristem at these transitional stages is not accessible by this method, and that fluorescent probes have to be applied by microinjection into the transitioning SAM itself.

In the present study we used low-current iontophoresis to investigate the symplasmic organization of the SAM during the transition to flowering. An additional advantage of this method is that it visualizes aspects of the symplasmic organization that are lost in ester-loading procedures. In the latter case the emerging picture is always a superposition of all transient plasmodesmal states over time (see *Discussion*).

In order to pinpoint the transition process precisely we selected an experimental system, mustard (*Sinapis alba* L.), in which flowering can be induced by exposure to a single LD. A single LD triggers the production of a floral stimulus in the leaves, which reaches the SAM at 16–28 h after the start of the LD. Leaf production by the SAM then ceases about 40 h after the start of the LD, and initiation of the first flowers at the terminal raceme eventually starts 1–1.5 days later (Bernier et al. 1967; Bernier 1989). Many cellular, biochemical and molecular changes that occur in the SAM during the first 3 days of the floral transition have been identified (Bernier 1989, 1997; Jacqmard et al. 1998), which makes it an excellent system to relate symplasmic alterations to subcellular changes. An event of particular interest for the present study is our previous finding that the Pd frequency is markedly increased in all SAM layers and zones from 28 to 48 h after the start of the LD (Ormenese et al. 2000), suggesting that the SAM is changing the properties of its symplasmic network during the transition to the inflorescence state. Here, we show that this is accompanied by a discrete change in the symplasmic coupling of the tunica cells, which results in a shift of the symplasmic balance between central zone cells and peripheral zone cells. We discuss how this shift might change the functional organization of the SAM in relation to its new function.

Materials and methods

Plant material

Plants of *Sinapis alba* L. were grown from seeds (Etablissement Jardins, Nancy, France) and kept vegetative under 8-h short days (SDs), as described by Lejeune et al. (1988). When the plants were 2–2.5 months old and approximately 25 cm tall, some of them were induced to flower by exposure to a single 22-h LD, which was followed by return to the regular 8-h SD regime. These plants will be referred to as "LD-induced". The "SD-control" plants were kept continuously under the standard 8-h SD conditions. During three independent experimentation periods, investigations were carried out with control plants and induced plants at two distinct stages of the floral transition. All light regimes were realized with V.H.O. Sylvania fluorescent white tubes with a photon flux density of 150 $\mu mol\ m^{-2}\ s^{-1}$, measured at the top of the plants. In a series of control experiments the effectiveness of the LD treatment in inducing the floral transition was tested. After 2 weeks all plants subjected to this LD had initiated flowers, whereas all plants that were kept continuously in SDs remained in the vegetative state.

Electrophysiology and iontophoresis

Procedures and methods

Experiments were carried out with SD-control plants during the daily light period at days 63–72 after sowing. Similar experiments were done with LD-induced plants during the first and second SDs following the inductive LD, that is, between 24 and 32 h or between 48 and 56 h after start of the LD, respectively (Fig. 1). The latter two kinds of induced plant will be referred to below as "LD-induced-day 1" and "LD-induced-day 2", respectively. Iontophoresis and electrophysiology were carried out as described earlier (van der Schoot and Lucas 1995; Rinne and van der Schoot 1998). The shoot apex of each plant was first gently defoliated, using a dissection microscope (Nikon, Tokyo, Japan), so that the SAM was well exposed (see Fig. 2a). The SAM was then immediately isolated from the shoot by sectioning the stem 3–4 mm below it, fixed with laboratory modeling clay in a transparent Plexiglas bathing chamber, and immediately submerged in tap water at room temperature. After a recovery time of 10–15 min, the bathing chamber was fixed on the stage of the fluorescence microscope (Optiphot II; Nikon, Tokyo, Japan). Subsequently, the SAM was inspected under low-irradiance white light in order to examine its outline and to check that the apical dome itself was not visibly damaged by the dissection procedure. It is important to note here that the majority of the *S. alba* SAMs, especially in SD-control plants, had a viscous surface due to the presence of external mucilage. This mucilage vanished progressively in LD-induced plants. Under epi-illumination with blue-violet (BV) and blue (B) lights, the SAM showed some red chlorophyll autofluorescence that outlined the overall shape of the apex. Excitation and barrier filters were standard BV and B filter-sets (BV: excitation 400–440/barrier 470/dichroic mirror 455; B: excitation 470–490/barrier 515/dichroic mirror 510). Glass microelectrodes were fabricated from borosilicate capillaries with an inner filament (World Precision Instruments, Sarasota, Fla., USA) on a horizontal pipette puller (PN-3; Narishige Scientific Instruments Laboratory, Tokyo, Japan). The tip diameters, approximately 0.5 μm, were capillary-filled with freshly made

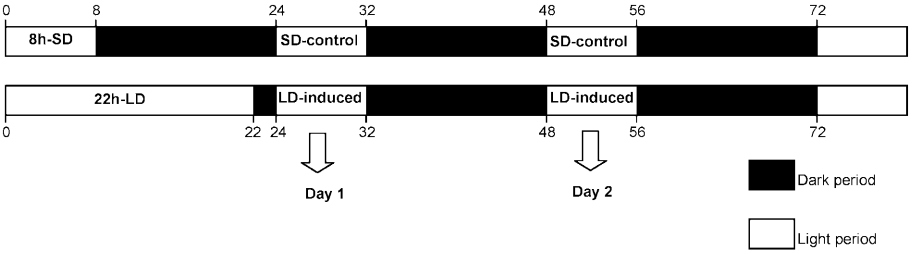

Fig. 1 Time-frame of the experiments. Numbers along the bars indicate hours after the start of the inductive LD. The *upper* diagram represents the control plants, kept continuously in the SD regime, and the *lower* diagram represents the plants induced by one 22-h LD before they returned to the SD regime. The microinjections were carried out in LD-induced plants during the first and the second SDs (*Day 1* and *Day 2*) following the inductive LD, and during the same days in corresponding SD-control plants (see *arrows*)

Lucifer Yellow CH solution (LYCH; 457 Da, 1% in distilled water). The micropipettes were then backfilled with 0.1 M KCl (1 M KCl in the holder) as an electrolyte. Finally, iontophoretic microinjection of a single SAM cell was carried out under the fluorescence microscope, using a hydraulic micromanipulator (MO-203; Narishige Scientific Instruments Laboratory) that was mounted on the stage of the microscope. Microinjections were aimed at a single superficial cell of the SAM centre, presumably a cell of the central zone. Microinjection in a cell of the SAM periphery was attempted but appeared technically difficult. It required the removal of the smallest leaf primordia that overarched the peripheral zone, a procedure that tended to result in meristem damage. Wounding of the SAM surface led to aberrant results, and therefore further microinjections into the peripheral part of the SAM were not pursued. The data of the three independent series of experiments were eventually pooled, as, due to the above difficulties, the number of successful experiments was relatively low. The overall, i.e. pooled, number of microinjected SAMs and the number of successful injections (in parentheses) were 180 (27), 90 (15) and 90 (22) for SD-control, LD-induced-day 1 and LD-induced-day 2 plants, respectively. The moderate success rate (15–17%) was predominantly due to the presence of charged mucilage.

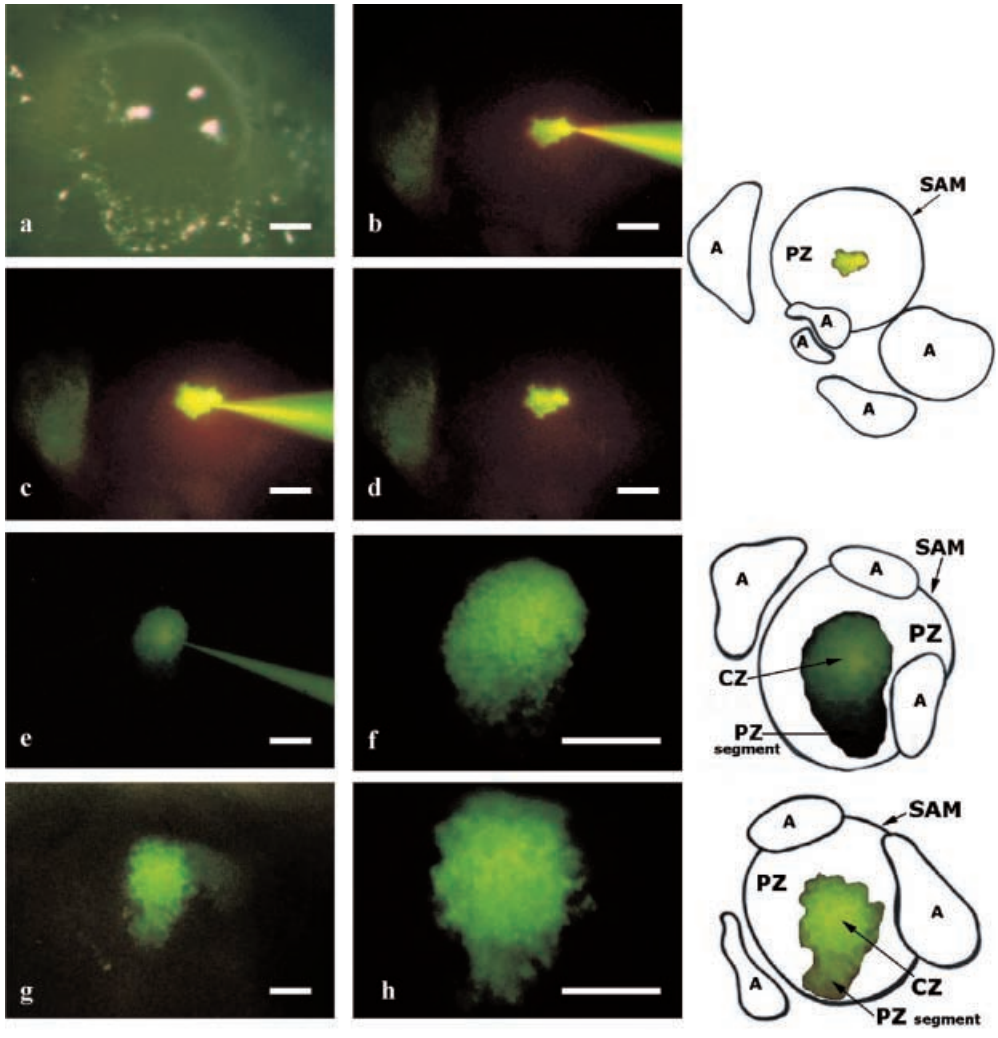

Fig. 2a–h Dye-coupling patterns in the vegetative SAM of *Sinapis alba* emerging after microinjection of a single central cell. In the diagrams, on the *right*, the position of the symplasmic field in the SAM is indicated in surface view. All structures surrounding the SAM are called appendages (*A*) regardless of whether they are leaves or stipules. *CZ* Central zone, *PZ* peripheral zone. **a** Surface view of an SD-control SAM under white light epi-illumination. **b** A triangular-shaped CSF; the microelectrode tip is in a cell. **c** About 5 min later than in **b** a second cell of the same CSF is microinjected. **d** After withdrawal of the microelectrode from the second impaled cell (see **c**) and an additional 10 min of waiting time, the CSF has maintained precisely the size and shape that emerged during the first microinjection. **e** LYCH moves symplasmically from cells of the CSF into a segment of the SAM periphery, thereby visualizing the presence of a ''fusion field''. **f** The same fusion field as in **e** 5 min after the microelectrode was drawn back from the impaled cell (higher magnification). **g** A fusion-field in another SAM. **h** The same field as in **g** at a higher magnification. Scale bars = 50 μm

Adsorption at the mucilage and diffusion into the cell walls

The physical contact of the microelectrode tip with the surface of the SAM could lead to an immediate adsorption of the negatively charged fluorescent dye (LYCH) from the tip to the positively charged mucilage. These SAMs exhibited a diffuse cloud-like fluorescence, with the LYCH equally adsorbed over the entire surface of the SAM. Even when this did not happen attempts to microinject were not always successful. The strong charges of the mucilage commonly prevented the recording of membrane potentials (E_m) and, as a result, the precise location of the microelectrode tip was often uncertain. In cases where the tip was in the cell walls, instead of in a cell, iontophoresis resulted in spread of LYCH in the cell walls. Hand-cut sections consistently confirmed that in both of these cases the dye was not located in the cells of the SAM and, consequently, these experiments were discarded.

Microinjection of a SAM cell

In the case of successful microinjections a sharp voltage drop signaled the entry of the microelectrode tip into a cell. Subsequent application of a small intermittent current (–3 to –6 nA) to the microelectrode then drove LYCH out of the electrode and into the impaled cell. This consistently resulted in the ready emergence of a central symplasmic field (CSF). LYCH outflow from the microelectrode tip into a cell, and the subsequent diffusion of the dye from cell to cell via open Pd, was monitored directly under the fluorescence microscope (see Figs. 2b, 3c). In all cases where a CSF was obtained, the tip of the microelectrode was drawn back from the impaled cell (see Fig. 3d) and subsequently a second cell of the same field (already containing the dye) was microinjected (see Figs. 2c, 3e). This double microinjection was used in order to check that the field kept the same size and shape when a cell at a different location in the field was microinjected. This appeared to be true in all cases. All these SAMs, with a CSF that retained a stable shape and distinct borders after the second microinjection (see Figs. 2d, 3f), were used in this study and listed in Table 1. The observations were documented and photographed (under BV, B, normal light or a combination of them) with a Nikon FX 35 WA/uFX-II camera system on Kodak Ektachrome 400 (super slide film; Kodak, Rochester, N.Y., USA) and reproduced in photographs and diagrams.

Measurement of surface areas of CSFs and whole SAMs

For each SAM listed in Table 1, a photograph was projected onto a screen at a fixed magnification of ×49, and the CSF was traced off using a transfer paper. Subsequently, the tracing off was scanned using an MFS-6000 CX scanner at a final magnification of ×980. The surface area of the projected CSF (*S*) was calculated using image-measurement software (SigmaScan Pro/Image; Jandel Scientific). Averages for the different SAM developmental stages were compared with a Student's *t*-test at the 5% level of significance using statistics software (SigmaStat; Jandel Scientific). In the case of non-normal populations, a

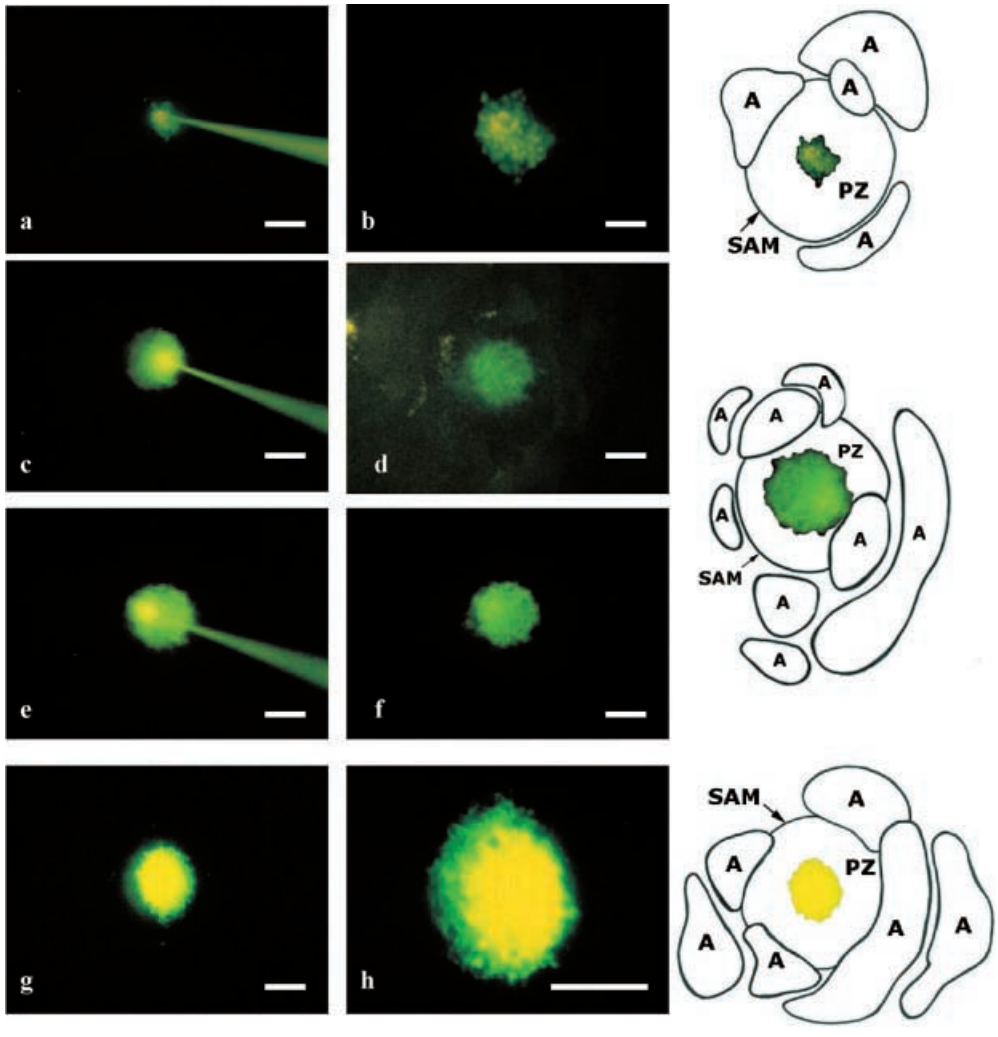

Fig. 3a–h Irregular and circular CSF emerging in LD-induced SAMs of *S. alba* after microinjection of a single central cell. In the diagrams, on the *right*, the position of the symplasmic field in the SAM is indicated in surface view. All structures surrounding the SAM are called appendages (*A*) regardless of whether they are leaves or stipules. *CZ* Central zone, *PZ* peripheral zone. **a** Irregular CSF of an LD-induced-day 1 SAM with the tip of the microelectrode in the impaled cell. **b** The CSF of **a** 5 min later, at higher magnification and with the microelectrode drawn back. The CSF shape and size are unchanged. **c** Circular CSF arising from a microinjected central cell of an LD-induced-day 1 SAM. **d** As in **c**, 3 min later, and with the microelectrode drawn back from the impaled cell; combined BV and white light. **e** About 5 min later a second cell of the same CSF, opposite to the first impaled cell, was microinjected. **f** After withdrawal of the microelectrode tip and an additional 10 min of waiting time, the field retained precisely the same size and shape as in **d** and **e**. **g** Circular CSF of an LD-induced-day 2 SAM. **h** As in **g**, but 5 min later, and at a higher magnification. Scale bars = 50 μm

Mann-Whitney Rank Sum test was used at the same level of significance. Considering that the dome-shaped SAM of *S. alba* L. is a part of a sphere (Bernier 1997), we calculated, for the different SAM stages, the surface area of the CSF in proportion to the SAM surface area, as:

$$P = \frac{\frac{r^2+h^2}{2h} - \sqrt{\left(\frac{r^2+h^2}{2h}\right)^2 - \frac{S}{\pi}}}{h} \quad (1)$$

in which S was the measured surface area of the projected CSF (as described above) and, r and h were the radius (width/2) and height of the SAM, respectively. Width was the line joining the axils of the two last-formed appendages in the most median SAM section and height the line perpendicular to the width passing through the SAM at its summit. The r and h values were obtained from Bernier (1997) who measured them in the same plant species, grown and induced to flower under identical environmental conditions.

Measurement of L1 cell width, height and circumference

Ten rapidly defoliated SAMs of both SD-control and LD-induced plants were collected at different time intervals after the start of the LD (24, 28, 32, 48 and 56 h) and fixed in 2% potassium permanganate in 0.2 M sodium cacodylate buffer (pH 7.4) for 45 min at 4 °C. After dehydration in a graded alcohol series, the SAMs were embedded in Epon. Three SAMs were randomly chosen from each batch. Ultrathin longitudinal axial sections (approximately 80–90 nm, pale silver interference color) were made in each SAM with a Sorvall MT-2 ultra-microtome. All the sections were collected on one-slot copper grids coated with 0.2% Formvar in chloroform, and subsequently contrasted for 3 min with 4.6% uranyl acetate solution in 50% ethanol. The sections were finally examined with a Zeiss EM 900 electron microscope at 80 kV. Six non-contiguous cells from each SAM were randomly selected in the entire L1 layer (four in the peripheral zone and two in the central zone). The lengths of the periclinal and anticlinal walls of each selected cell were measured on electron micrographs at the final magnification of ×20,000 using image-measurement software (SigmaScan Pro/Image; Jandel Scientific), and a video editor and capture program (Video Studio 2; Ulead Systems). Values obtained for anticlinal and periclinal walls of central and peripheral cells were averaged for each collection time and pooled for each SAM developmental stage. Periclinal wall lengths (i.e. cell width), anticlinal wall lengths (i.e. cell height), and calculated cell circumferences at the different SAM stages were then compared with a Student's *t*-test at the 5% level of significance using the same statistics software as above.

Table 1 Numbers of experiments (n) and proportions of CSFs with various shapes in the SAM of SD-control and LD-induced plants of *Sinapis alba*

SAM developmental stage	n	Proportion of CSF of different shape
SD-control	27	
LD-induced-day 1	15	
LD-induced-day 2	22	

Results

Aim of the investigations and experimental approach

Plasmodesmal frequencies in the SAM of *S. alba* L. increase considerably during the floral transition (Ormenese et al. 2000). This suggests that signal coupling as well as metabolic coupling between SAM cells is subject to change when the SAM assumes its new role in plant development. In addition, the spatial organization of the symplasmic space in the SAM may change in correspondence to the newly acquired developmental tasks of the SAM. Experimentally we addressed the latter possibility by asking two main questions: (i) Is the expanding symplasmic space of the tunica in the SAM of *S. alba* dynamically and iteratively organized into a central and a peripheral part, like in other plant species, and, if so, (ii) is the balance between the central and the peripheral parts subject to alteration during the floral transition, considering that different appendages are formed in an altered phyllotactic pattern?

The symplasmic organization of the vegetative SAM

To map the patterns of dye-coupling between SAM cells we employed the technique of iontophoretic microinjection (Rinne and van der Schoot 1998; Rinne et al. 2001). Entry of the microelectrode into a single SAM cell is monitored electrically. The advantage is that the intracellular location of the tip is certain, and that the subsequent injection of dye is known to be inside that same cell. The *S. alba* SAM presented an experimental difficulty which deserves some attention as a background for the experiments. The *S. alba* SAM frequently possessed a strongly charged mucilage at the surface of the SAM which could prevent the successful recording of a membrane potential. In these experiments, cell impalement was carried out visually, as is the practice with pressure injection (e.g. van der Schoot and Lucas 1995; Storms et al. 1998). The tip (diameter in the sub-micron range) could be inside an L1 cell or in a cell of the second layer, which in *S. alba* is the second tunica layer (Bernier 1962). Once the dye was microinjected, the SAMs invariably displayed in a matter of seconds the presence of a centrally located field of dye-coupled cells. The presence and position of this CSF corresponded to similar CSFs observed in the SAMs of other plant species (Rinne and van der Schoot 1998; van der Schoot and Rinne 1999b). Second microinjections in a different cell of the same CSF, already possessing the dye, were performed routinely. Invariably, this procedure intensified the fluorescence of the CSF, but never resulted in an alteration in CSF shape or size (Fig. 2b–d). It is possible that only one, not both, of the injections was in the L1 layer. If so, this obviously did not change CSF shape and size, indicating that the field in the L1 is similar to that in the L2, or that the CSF includes both tunica

layers. This robustness of the CSFs in *S. alba* SAMs permitted a more systematic investigation of the geometry of the fields as observed in surface view.

Change in field geometry during the floral transition

The shape and size of CSFs in the SAM were studied in three developmental stages: one vegetative state, and two induced states (LD-1 and LD-2). The CSFs could be classified according to their geometrical proportions into three categories: triangular (Fig. 2b–d), irregular (Fig. 3a, b) and circular (Fig. 3c–h). The triangular fields were the smallest and the circular fields were the largest. At the vegetative stage the SAM displayed predominantly small and triangular CSFs (55.5%), although some were somewhat larger and irregular (29.5%), and some were large and circular (15%; Table 1). After exposure to a single LD the proportion of these categories changed. At the first stage after exposure, which is LD-1, triangular CSFs were strongly reduced in number (13.5%) whereas irregular CSFs and circular fields increased strongly (53% and 33.5%, respectively). At the second stage after LD exposure, which is LD-2, the proportion of triangular CSFs remained at a low level (18%), whereas irregular CSFs had decreased considerably (23%) and the circular CSFs increased (59%). In summary, after exposure to a single LD, triangular-shaped CSFs were replaced – via an intermediate irregular stage – with circular-shaped CSFs. In the vegetative state, but not in the induced states, 6.9% of the total number of successful experiments showed 'fusion fields', in which the CSF was fused with a segment of the peripheral field (Fig. 2e–h).

Increase in CSF size at the floral transition

The SAM of *S. alba* responded to the application of an inductive LD by increasing the average surface area (*S*) of its CSF more than 3-fold in 2 days (Table 2). The surface area of CSFs increased irrespective of their shape (Fig. 4). Interestingly, the same pattern was observed at each developmental stage of the SAM: triangular CSFs were the smallest and circular CSFs (or in one case irregular) were the largest. The differences in shape were not due to variation in size, but represented real geometric changes.

Table 2 Average (± SE) radii (*r*) and heights (*h*) of the *S. alba* SAM dome, surface areas of the projected CSFs (*S*) and CSF surface areas as proportions of total surface areas of the SAM dome (*P*), at the different SAM stages

SAM developmental stage	*r* (μm)	*h* (μm)	*S* (μm^2)	*P* (%)
SD-control	79.8 ± 1.9	33.9 ± 1.5	2.904 ± 490	13
LD-induced-day 1	81.9 ± 3.5	34.9 ± 4.8	8.256 ± 1744	35
LD-induced-day 2	97.4 ± 4.6	49.3 ± 9.0	9.536 ± 1288	27

Given that the surface of the SAM is curved, and CSF surface areas (*S*) were measured from photographs as projections (see *Materials and methods*), the increase in *S* values at the floral transition resulted in an underestimation. To correct for these errors we had to assess both the size and curvature of the SAM dome for the different developmental stages that were investigated. To calculate the proportion of the total surface area of the SAM dome occupied by the CSF (*P*) the SAM radii (*r*) and heights (*h*) were obtained and substituted into Eq. 1. Data in Table 2 indicate that the SAM *r* and *h* were similar during day 1 in induced plants and in SD-control plants. In contrast, both *r* and *h* increased during day 2 in induced plants. Thus, the size of the SAM increased only on day 2. On day 1, the proportion of the SAM surface occupied by the CSF in induced plants exhibited an almost 3-fold increase. Later, on day 2, the relative CSF increase was less, apparently because the SAM size (and thus the SAM surface) was now increasing. In summary, during the initial stage of the floral transition the CSF at the summit of the dome increased rapidly in absolute size, whereas the dome itself did not. The dome started to expand only later, particularly outside the CSF, resulting in a proportional increase in the peripheral part of the SAM where a new kind of appendage will start to form.

Increased CSF area and SAM size at floral transition are not caused by cell enlargement

In order to assess whether the increases in CSF area and SAM size (Table 2) were due to cell enlargement, extra cell divisions, or both, we measured in SAM longisections the lengths of periclinal cell walls (cell width), anticlinal cell walls (cell height) and the circumference of the L1 cells at the three SAM stages examined (Fig. 5). It appeared that the average width, height (data not shown) and circumference of L1 cells did not show any statistically significant change during the transition to

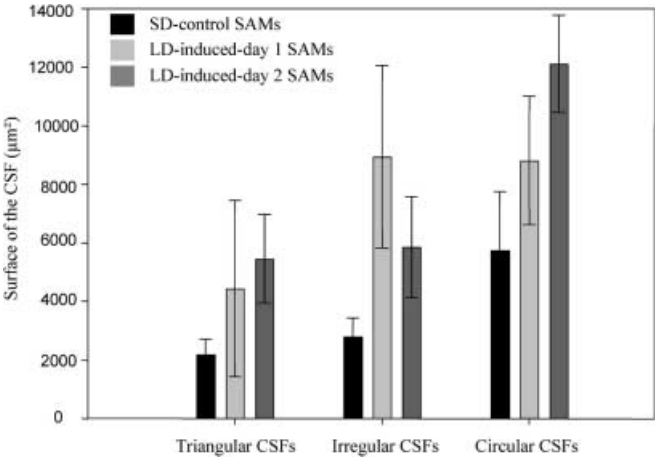

Fig. 4 Surface areas (± SE) of the projected triangular, irregular or circular CSFs at the three investigated developmental stages of the *S. alba* SAM

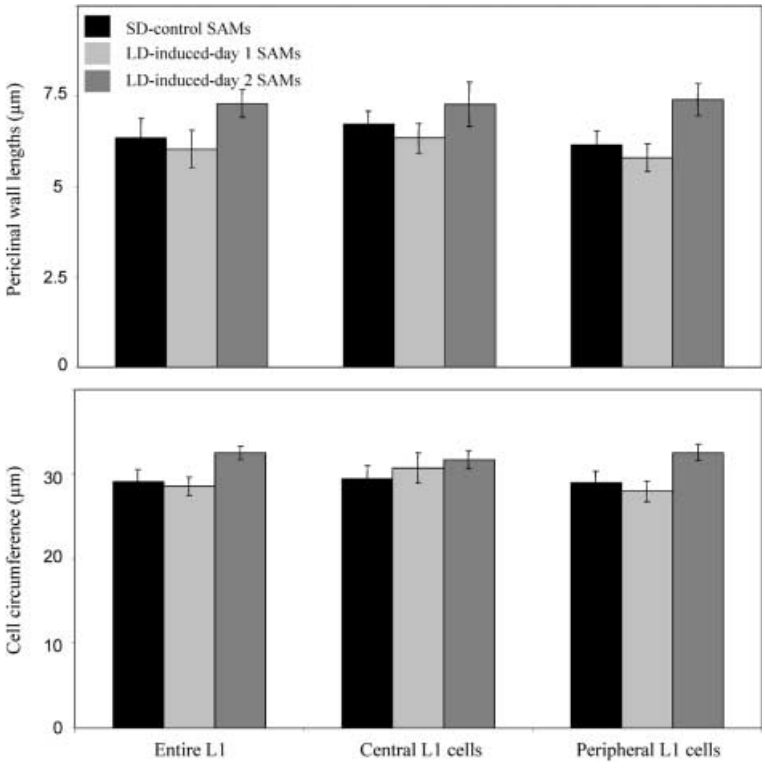

Fig. 5 Circumference and periclinal wall length (± SE) of cells in the first layer (L1) within the L1 layer, within the central zone, and within the peripheral zone of the *S. alba* SAM. Values are given for the three investigated developmental stages

flowering. To rule out the possibility that cells within the L1 centre had become bigger while those in the periphery had become smaller or vice versa, we also measured cells in the centre and periphery separately (Fig. 5). It appeared that there was no statistically significant difference in these cell parameters, either between the centre and periphery of the L1 layer at any of the three developmental stages of the SAM, or between the SAM of these different stages. Therefore, cellular volumes in L1 were constant during the first 2 days of the floral transition, and increases in CSF area and SAM size could not be ascribed to cell enlargement. Instead, they appeared to be exclusively due to increases in the number of cells within the boundaries of the CSF and the SAM, respectively.

Discussion

The functioning of the SAM as an integrated developmental unit is dependent on the exchange of correlative signals between its cells as well as on the import of nutrients and their internal distribution. During the transition to flowering the number of plasmodesmal connections in the SAM strongly increases (Ormenese et al. 2000), thereby potentially intensifying supply from the subtending stem as well as radial signalling between the centre and the periphery of the SAM to support the formation of a new kind of lateral appendage. Here, we have experimentally addressed the latter problem, asking the question of whether the radial symplasmic organization of the SAM is altered during the floral transition, when new structures arise at the periphery of the meristem. Since the tunica is the route par excellence for radial signalling we focused our experiments on the symplasmic organization of the tunica and the way it is altered during the floral transition.

In any investigation the choice of techniques influences the way the problem is formulated and the kind of information that is obtained. As various techniques have become available for investigating the symplasmic space in plants, we will first evaluate the possibilities and limitations that are inherent to these techniques and motivate our choice.

Technical possibilities and limitations.

In recent years the general picture that the majority of Pd allow the diffusional passage of small molecules up to 1 kDa (Lucas et al. 1993) has been questioned. The size exclusion limit (SEL), commonly measured in source leaves, appeared to be very different in sink areas. GFP (27 kDa) and GFP-fusion proteins (50–60 kDa), expressed behind the companion-cell-specific promoter *AtSUC2*, appeared to move through Pd into the sieve tubes and out into sink leaves (Imlau et al. 1999; Oparka et al. 1999). Their movement followed photosynthetic influx, and correlated with a linear Pd morphology (Oparka et al. 1999). Crawford and Zambryski (2000, 2001) showed, in addition, that subcellular localization is a determining factor, and that even in source leaves a small percentage of cells permitted the diffusion of GFP to adjacent cells.

The discrepancy with earlier observations on the Pd SEL might be due to several factors. In the case of microinjection the SEL is influenced by the choice of the tissue, tissue preparation, cell impalement, and the method by which the probes are driven into the cell. In most cases, researchers used source leaves for microinjection, as sink leaves are small and difficult to strip. Experiments with real sink leaves would probably have shown their large SEL. Stripping the epidermis damages cells to some extent, leading to SEL values that are much too low. Similarly, cell impalement with a microelectrode can damage a cell and lead to an underestimation of the SEL, particularly in cells with high turgor. Neither problem arises in the case of SAM injections because the SAM is not stripped, and its cells have not yet developed a central vacuole to build-up turgor.

Introducing a volume of liquid into a target cell creates a pressure difference over the Pd and might narrow them (Oparka and Prior 1992; Storms et al. 1998). In small cells, like those of the SAM, the side effect of pressure injection (van der Schoot and Lucas 1995) is even more likely to occur. Iontophoretic injection with currents that hyperpolarize the cell membrane beyond physiological values can also damage the cell and lead to erroneous SEL values. Both factors have contributed to the confusion that surrounds these techniques. In the case of low-current iontophoresis this problem is avoided, and the state of the cell can be monitored through the membrane potential (see *Materials and methods*). Apart from this, it should be pointed out that the SEL values are not measured in the present study, as the goal was to investigate possible changes in patterns of cell coupling rather than cell coupling as such.

Studies with transgenic plants that produce fluorescent proteins behind a tissue- or cell-specific promoter, like for example GFP (Imlau et al. 1999; Oparka et al. 1999), provide a welcome addition to the spectrum of investigations. Such plants show that sink leaves can ''take in'' large molecules by diffusion through Pd. The inherent limitations of this method are that only those tissues are reached that are symplasmically connected to the phloem by dilated Pd (Crawford and Zambryski, 1999), and that the fluorescence distribution reflects the superposition of all possible Pd states between the phloem and these tissues. In other words, the method does not discriminate in time. Import of ester-loaded dyes into the SAM has similar limitations. In the case of the present study, import of dyes from the shoot system is no option as the transitioning SAM of *Arabidopsis* is symplasmically isolated (Gisel et al. 1999). This indicates that in *Sinapis*, as in *Arabidopsis*, direct low-current iontophoretic microinjection into target cells of the SAM is at present the obvious method to study the floral transition.

A central symplasmic field (CSF)

Low-current iontophoretic microinjection shows that, in *S. alba*, the SAM possesses a CSF (Fig. 2b–d), like in birch (Rinne and van der Schoot 1998; Rinne et al. 2001) and potato (van der Schoot and Rinne 1999b). Open Pd interconnected all the cells of this CSF, since LYCH rapidly diffused from the injected cell to all the other cells within the CSF. Because LYCH remains confined to the cells of the field its outer cells must have their Pd narrowed or closed at the interface between them and the cells outside the field. The cells at the centre of the SAM are thus symplasmically separated from those at the periphery, as in the other species mentioned above. However, in 6.9% (Table 2) of the vegetatively growing plants the CSF fused with a segment of the SAM periphery, suggesting that during plastochronic progression there is a narrow time window during which signals can traffic symplasmically between the SAM centre and periphery. In birch seedlings a similar symplasmic corridor is present during a narrow plastochronic window (7.9%; Rinne and van der Schoot 1998). The temporary symplasmic corridor might be used to traffic various kinds of morphogenetic signal. These signals might, for example, serve the establishment of a group of founder cells, as suggested by Scanlon (2000), the development of future dorsiventrality in incipient leaf primordia (Steeves and Sussex 1989), or the transmission of florigenic signals (Rinne and van der Schoot 1998). In the latter case it is of interest that, for example, in *Anagallis* the SAM is only competent to respond to an inductive photoperiod during a short time window in its plastochronic trajectory (Bernier 1988).

The shape of the CSF in the vegetative *S. alba* SAM is often triangular, and occupies a relatively small fraction of the SAM surface (Tables 1, 2; Fig. 2b–d). That the shapes and sizes of the CSF are genuine was established by routinely performing second injections in cells that were already dye-coupled. If shape and size simply result from the amount of injected dye the additional injections of LYCH would have resulted in a further increase in the CSF. This was never observed, however. The only change that took place during the second injection was an increase in the intensity of the fluorescent signal in all cells of the CSF. This shows that the boundaries of the CSFs are robust. The individual CSFs therefore, must represent the true shape of the field that was present in a particular SAM.

Geometric alterations to the CSF during the floral transition

A clear tendency is present in the way the geometry of the CSF changes during the floral transition: the vegetative SAM of *S. alba* is dominated by triangular CSFs whereas the SAM of induced plants at day 2, which is about 1 day prior to visible formation of flower primordia, possesses mostly circular CSFs (Table 1). The possibility that each CSF shape relates to a particular stage of the plastochron is very unlikely in a plant such as *S. alba* because it has a spiral phyllotaxis and thus all plastochron stages occur simultaneously in different

sectors of the SAM peripheral zone. In the vegetative SAM of potato the CSF is composed of cellular subgroups that correspond precisely to the number of initial cells (van der Schoot and Rinne 1999b). This strongly suggests that the three subgroups are clonal sectors that are produced by the three centrally located initial cells. Given the number and arrangement of the clonal subfields – the ends tapering towards the future primordia sites – their constellation might reflect and influence phyllotaxis. In the case of the three subfields in potato the CSF as a whole has a triangular geometry. When more than three subfields are present – that is more than three initial cells – the CSF as a whole might be star-shaped, or smoothed out into a circular shape. In *S. alba* the alteration of CSF geometry at the floral transition could possibly reflect an increase in the complexity of phyllotaxis. That *S. alba* phyllotaxis is indeed altered during the floral transition was shown in a previous study (Bernier 1997). Thus, although the phyllotactic system at both the vegetative and inflorescence stages is spiral, it becomes more complex at the inflorescence stage, as indicated by the fact that the phyllotaxis index (Williams 1975) rises from 2.9 in the vegetative SAM to 3.9 in the inflorescent SAM. In this scenario, the intervening phase on day 1, in which most CSFs are irregular in shape (Table 1), might represent a transient reorganization phase during which the 'positional coordinates' at the SAM are reset and a new geometry is established.

If this theoretical consideration is correct, the small number of SAMs of SD-control plants exhibiting irregular or circular CSFs must then be viewed as undergoing the precocious and autonomous shift to a more complex phyllotaxis while remaining vegetative. The small number of SAMs of the LD-induced plants that still exhibit a triangular CSF are likely those of plants that lag behind the fast-responding plants (Bernier 1989).

The CSF size increases during floral transition and this is due to an increased cell number

During the first phase of the shift to flowering, the CSF enlarges its size by almost 3-fold (Table 2), and this increase is not only absolute, but also in proportion to the size of the SAM. In addition, the increase in CSF size precedes the enlargement of the SAM domes by 1 day. This shows that the CSF enlargement is independent of the scaling up of the SAM size, and that the CSFs increase their share in the top layer of the SAM. This changes the spatial relation between the centre and periphery of the SAM. Theoretically, it also implies that the mechanisms that control the size of the CSF are altered at the floral transition. It has been proposed that the initial cells of the CSF could gradient-wise determine at which location in the SAM the boundary of the CSF is formed (Rinne and van der Schoot 1998). In this model the increased production of the active factor by the initial cells could lead to enlargement of the CSF because the threshold level that triggers Pd closure would become displaced from the initials towards the periphery of the SAM.

Our analyses of size parameters in L1 cells (Fig. 5) show that the increase in CSF size during the transition is exclusively due to an increase in the number of cells. The data rule out the possibility that cell stretching is the cause of the CSF increase since, in the periphery as well as in the centre of the SAM, L1 cells retain exactly the same size. Thus the CSF as a metabolic compartment increases its volume and, potentially, its capacity to produce metabolites and/or morphogens. On day 2 the surface area of the CSF proportionally decreases (Table 2). The CSF surface area is still increasing but the SAM dome surface (and volume) has also started to increase, causing a shift in the balance of the number of cells in the CSF and in the SAM as a whole. Apparently, the enlarging CSF more rapidly releases cells to the periphery of the SAM for recruitment by the emerging flower primordia, about 1 day later.

Changing CSF and gene expression during floral transition

Interestingly, during day 1, at the time the CSF is changing its shape and increasing its size, the *SaMADSA* gene starts to be expressed in the central corpus (L3) cells of the SAM (Bonhomme et al. 2000). *SaMADSA* is believed to be a critical gene for floral evocation in *S. alba* since (i) it is the ortholog of the *A. thaliana SOC1* gene, which is considered as a part of a transcriptional cascade ultimately leading to activation of the floral meristem identity genes *LFY* and *AP1*, in the SAM (Borner et al. 2000; Lee et al. 2000; Samach et al. 2000); and (ii) constitutive expression of *SaMADSA* greatly hastens flowering in *A. thaliana* in both LDs and SDs and causes photoperiod-independent flowering in the strict SD plant Maryland Mammoth tobacco (Bonhomme et al. 2000; Borner et al. 2000).

The fact that the changes in shape and size of the CSF occur approximately simultaneously with the up-regulation of a critical evocational gene is probably not fortuitous. Temporal coordination of the two events might be essential for the completion of floral evocation, as activation of *SaMADSA* alone is insufficient to bring about the floral transition (Bonhomme et al. 2000). In addition, spatial coordination of events across the SAM might be critical since the up-regulation of *SaMADSA* occurs in the central L3 cells located just beneath the cells of the changing CSF. The importance of such spatial coordination has been demonstrated in the case of the *CLAVATA1-3* (*CLV1-3*) and *WUSCHEL* (*WUS*) genes in *A. thaliana* (e.g. Fletcher and Meyerowitz 2000; Schoof et al 2000). *CLV3* is expressed in the central cells of both tunica layers, whereas *CLV1* mRNA is found only in the underlying corpus cells. Genetic analyses indicate that *CLV1* and *CLV3* function in the same pathway to regulate cell proliferation in the central areas of tunica and corpus. Interestingly, *clv1* and *clv3*

mutations both result in an oversized meristem with a characteristically enlarged central zone. This indicates, firstly, that the tunica and the corpus cooperate in maintaining the size of the central zone, and secondly, that in the case of *clv1* or *clv3* mutants, cell-exit from the central zone is reduced (see Laufs et al. 1998; Fletcher and Meyerowitz 2000). The term exit underlines that the cells in the central zone are somehow united. This requires a mechanism that is spatially extended, and which is "stretched out" in *clv1* and *clv3* mutants. This mechanism could be a gradient field or, in view of the present results, a symplasmic field that is controlled by a gradient. It seems imperative, therefore, to investigate the potential role of genes like *CLV1-3* and *WUS* in the floral shift of *S. alba* in the context of alterations in symplasmic fields as demonstrated here.

Acknowledgements The authors are grateful to Dr. R. Deltour for critical reading of the manuscript and to R. Marquet for his help with the mathematical aspects of the work. This work was supported by grants from the Interuniversity Poles of Attraction Programme (Belgian State, Prime Minister's Office – Federal Office for Scientific, Technical and Cultural Affairs; P4/15) and the University of Liège (Fonds Spéciaux). S.O. is grateful to F.R.I.A. for the award of a research fellowship. Other support to S.O. was provided by grants from the F.N.R.S. and the Royal Academy of Sciences of Belgium.

References

Bergmans ACJ, de Boer D, van Bel AJE, van der Schoot C (1993) The initiation and development of *Iris* flowers – permeability changes in the apex symplasm. Flowering Newslett 16:19–25

Bergmans ACJ, de Boer AD, Derksen JWM, van der Schoot C (1997) The symplasmic coupling of L2-cells diminishes in early floral development. Planta 203:245–252

Bernier G (1962) Evolution of the apical meristem of *Sinapis alba* L. (long-day plant) in long days, in short days and during the transfer from short days to long days. Caryologia 15:303–325

Bernier G (1988) The control of floral evocation and morphogenesis. Annu Rev Plant Physiol Plant Mol Biol 39:175–219

Bernier G (1989) Events of the floral transition of meristems. In: Lord E, Bernier G (eds) Plant reproduction: from floral induction to pollination. American Society of Plant Physiologists Series, vol I, Rockville, Maryland, pp 42–50

Bernier G (1997) Growth changes in the shoot apex of *Sinapis alba* during transition to flowering. J Exp Bot 48:1071–1077

Bernier G, Kinet J-M, Bronchart R (1967) Cellular events at the meristem during floral induction in *Sinapis alba* L. Physiol Veg 5:311–324

Bonhomme F, Kurz B, Melzer S, Bernier G, Jacqmard A (2000) Cytokinin and gibberellin activate *SaMADS A*, a gene apparently involved in regulation of the floral transition in *Sinapis alba*. Plant J 24:103–111

Borner R, Kampmann G, Chandler J, Gleißner R, Wisman E, Apel K, Melzer S (2000) A MADS domain gene involved in the transition to flowering in *Arabidopsis*. Plant J 24:591–599

Carpenter R, Coen ES (1995) Transposon induced chimeras show that *floricaula*, a meristem identity gene, acts non-autonomously between cell layers. Development 121:19–26

Crawford KM, Zambryski PC (1999) Plasmodesmata signaling: many roles, sophisticated statutes. Curr Opin Plant Biol 2:382–387

Crawford KM, Zambryski PC (2000) Subcellular localization determines the availability of non-targeted proteins to plasmodesmal transport. Curr Biol 10:1032–1040

Crawford KM, Zambryski PC (2001) Non-targeted and targeted protein movement through plasmodesmata in leaves in different developmental and physiological states. Plant Physiol 125:1802–1812

Fletcher JC, Meyerowitz EM (2000) Cell signaling within the shoot meristem. Curr Opin Plant Biol 3:23–30

Gisel A, Barella S, Hempel FD, Zambrisky PC (1999) Temporal and spatial regulation of symplastic trafficking during development in *Arabidopsis thaliana* apices. Development 126:1879–1889

Goodwin PB, Lyndon RF (1983) Synchronisation of cell division during transition to flowering in *Silene* apices not due to increased symplast permeability. Protoplasma 116:219–222

Hantke SS, Carpenter R, Coen ES (1995) Expression of *floricaula* in single cell layers of periclinal chimeras activates downstream homeotic genes in all layers of floral meristems. Development 121:27–35

Hartmann U, Höhmann S, Nettesheim K, Wisman E, Saedler H, Huijser P (2000) Molecular cloning of *SVP*: a negative regulator of the floral transition in *Arabidopsis*. Plant J 21:351–360

Hempel FD, Weigel D, Mandel MA, Ditta G, Zambryski PC, Feldman LJ, Yanofsky MF (1997) Floral determination and expression of floral regulatory genes in *Arabidopsis*. Development 124:3845–3853

Imlau A, Truernit E, Sauer N (1999) Cell-to-cell and long distance trafficking of the green fluorescent protein in the phloem and symplastic unloading of the protein into sink tissues. Plant Cell 11:309–322

Jacqmard A, Houssa C, Bernier G (1998) Control of the cell division cycle changes in the shoot meristem of *Sinapis alba* during the transition to flowering. In: Bryant JA, Chiatante D (eds) Plant cell proliferation and its regulation in growth and development. Wiley, New York, pp 67–78

Jackson D, Veit B, Hake S (1994) Expression of maize *KNOTTED1* related homeobox genes in the shoot apical meristem predicts patterns of morphogenesis in the vegetative shoot. Development 120:405–413

Kania T, Russenberger D, Peng S, Apel K, Melzer S (1997) FPF1 promotes flowering in *Arabidopsis*. Plant Cell 9:1327–1338

Laufs P, Grandjean O, Jonak C, Kieu K, Traas J (1998) Cellular parameters of the shoot apical meristem in *Arabidopsis*. Plant Cell 10:1375–1389

Lee H, Suh S-S, Park E, Cho E, Ahn JH, Kim S-G, Lee JS, Kwon YM, Lee I (2000) The AGAMOUS-LIKE 20 MADS domain protein integrate floral inductive pathways in *Arabidopsis*. Genes Dev 14:2366–2376

Lejeune P, Kinet J-M, Bernier G (1988) Cytokinin fluxes during floral induction in the long day plant *Sinapis alba* L. Plant Physiol 86:1095–1098

Lucas WJ, Ding B, van der Schoot C (1993) Plasmodesmata and the supracellular nature of plants. New Phytol 125:435–476

Lucas WJ, Bouché-Pillon S, Jackson DP, Nguyen L, Baker L, Ding B, Hake S (1995) Selective trafficking of KNOTTED1 homeodomain protein and its mRNA through plasmodesmata. Science 270:1980–1983

Lyndon RF (1998) The shoot apical meristem: its growth and development. Cambridge University Press, Cambridge

Nougarède A (1967) Experimental cytology of the shoot apical cells during vegetative growth and flowering. Int Rev Cytol 21:203–251

Oparka KJ, Prior DAM (1992) Direct evidence for pressure-generated closure of plasmodesmata. Plant J 2:741–750

Oparka KJ, Roberts AG, Boevink P, Santa Cruz S, Roberts I, Pradel KS, Imlau A, Kotlizky G, Sauer N, Epel B. (1999) Simple, but not branched, plasmodesmata allow the non-specific trafficking of proteins in developing tobacco leaves. Cell 97:743–754

Ormenese S, Havelange A, Deltour R, Bernier G (2000) The frequency of plasmodesmata increases early in the whole shoot apical meristem of *Sinapis alba* L. during floral transition. Planta 211:370–375

Perbal M-C, Haughn G, Saedler H, Schwarz-Sommer Z (1996) Non-cell-autonomous function of the *Antirrhinum* floral

homeotic proteins DEFICIENS and GLOBOSA is exerted by their polar cell-to-cell trafficking. Development 122:3433–3441
Ratcliffe OJ, Bradley DJ, Coen ES (1999) Separation of shoot and floral identity in *Arabidopsis*. Development 126:1109–1120
Rinne PLH, van der Schoot C (1998) Symplastic fields in the tunica of the shoot apical meristem coordinate morphogenetic events. Development 125:1477–1485
Rinne PLH, Kaikuranta PM, van der Schoot C (2001) The shoot apical meristem restores its symplasmic organization during chilling-induced release from dormancy. Plant J 26:249–264
Samach A, Onouchi H, Gold SE, Ditta GS, Schwarz-Sommer Z, Yanofsky MF, Coupland G (2000) Distinct roles of CONSTANS target genes in reproductive development of *Arabidopsis*. Science 288:1613–1616
Sawhney VK, Rennie PJ, Steeves TA (1981) The ultrastructure of the central zone cells of the shoot apex of *Helianthus annuus*. Can J Bot 59:2009–2015
Scanlon MJ (2000) Developmental complexities of simple leaves. Curr Opin Plant Biol 3:31–36
Schoof H, Lenhard M, Haecker A, Mayer KF, Jurgens G, Laux T (2000) The stem cell population of *Arabidopsis* shoot meristems is maintained by a regulatory loop between the *CLAVATA* and *WUSHEL* genes. Cell 100:635–644
Sessions A, Yanofsky MF, Weigel D (2000) Cell-cell signaling and movement by the floral transcription factors *LEAFY* and *APETALA1*. Science 289:779–781
Steeves TA, Sussex IM (1989) Patterns in plant development, 2nd edn. Cambridge University Press, Cambridge
Storms MMH, van der Schoot C, Prins M, Kormelink R, van Lent JWM, Goldbach RW (1998) A comparison of two methods of microinjection for assessing altered plasmodesmal gating tissues expressing viral movement proteins. Plant J 13:131–140
van der Schoot C, Lucas WJ (1995) Microinjection and the study of tissue patterning in plant apices. In: Maliga P, Klessing DF, Cashmore AR, Gruisem W, Varner JE (eds) Methods in plant molecular biology. Cold Spring Harbor Laboratory Press, Cold Spring Harbor, NY, pp 173–189
van der Schoot C, Rinne PLH (1999a) The symplasmic organization of the shoot apical meristem of angiosperms. In: van Bel AJE, van Kesteren WJP (eds) Plasmodesmata. Structure, function, role in cell communication. Springer, Berlin Heidelberg New York, pp 225–242
van der Schoot C, Rinne PLH (1999b) Networks for shoot design. Trends Plant Sci 4:31–37
Williams RF (1975) The shoot apex and leaf growth. Cambridge University Press, Cambridge